Bioorganic & Medicinal Chemistry xxx (2015) xxx–xxx

Contents lists available at ScienceDirect

Bioorganic & Medicinal Chemistry

journal homepage: www.elsevier.com/locate/bmc

Synthesis and evaluation of selegiline derivatives as monoamine oxidase inhibitor, antioxidant and metal chelator against Alzheimer's disease

Shishun Xie, Jie Chen, Xiruo Li, Tao Su, Yali Wang, Zhiren Wang, Ling Huang *, Xingshu Li *

Institute of Drug Synthesis and Pharmaceutical Process, School of Pharmaceutical Sciences, Sun Yat-sen University, Guangzhou 510006, China

ARTICLE INFO

Article history:
Received 19 January 2015
Revised 1 April 2015
Accepted 2 April 2015
Available online xxxx

Keywords:
Monoamine oxidase inhibitor
Metal chelator
Alzheimer's disease

ABSTRACT

A series of compounds with monoamine oxidase inhibition and biometal chelation activities were designed, synthesised and evaluated as agents against Alzheimer's disease. The in vitro assay shows that most target compounds exhibit good MAO-B activities with submicromolar IC_{50} values and antioxidant activity (1.49–5.67 ORAC-FL values). The selected compounds were used to determine the biometal chelating ability using UV–vis spectrometry and high-resolution mass spectrometry, which confirm that they can effectively interact with copper(II), iron(II) and zinc(II). The ThT fluorescence binding assay indicates that the synthetic compounds can inhibit Cu(II)-induced $A\beta_{1-42}$ aggregation. The parallel artificial membrane permeation assay shows that most target compounds can cross the BBB. Based on these results, compound **8a** was selected as a potential multifunctional agent for the treatment of AD.

1. Introduction

Alzheimer's disease (AD) is a fatal neurodegenerative disorder that affects more than 24 million people worldwide, and there is no effective treatment, although more than 100 years have passed since its discovery.[1] At present, the main clinical treatment strategy for AD is the use of cholinesterase inhibitors such as donepezil, rivastigmine, and galantamine.[2] It is believed that these drugs modestly improve the memory and cognitive function but do not prevent progressive neurodegeneration because of the complexity of AD pathogenesis. In the past decades, some hallmarks such as low levels of acetylcholine, oxidative stress, β-amyloid (Aβ) deposits, τ-protein aggregation, dyshomeostasis of biometals and inflammation have been found to play important roles in the pathogenesis of AD.[3] Based on these discoveries, many different approaches to treat AD have been developed. In particular, the multi-target-directed ligand (MTDL) strategy, which incorporates a sequential, multifactorial approach to this multifaceted disease, has received much attention.[4]

Studies indicate that the dysregulation of brain metal-ion homeostasis, particularly that of copper, iron and zinc, is an important hallmark of AD.[5] These metal levels increase from 3 to 5 fold in AD brains compared to those in age-matched controls.[6] Zinc(II) and copper(II) are significantly enriched in plaque amyloid and are coordinated with histidine residues in senile plaque (SP) cores, which was confirmed using Raman microscopy.[7] Because these biometal ions may be crucial participants in AD pathological processes, the modulation of these biometals was proposed to be a potential therapeutic strategy to treat this disease. Actually, clioquinol and its analogue PBT2, an 8-OH quinoline derivative, which exhibit rapid restoration of cognition in Alzheimer's transgenic mice associated with decreased interstitial Aβ,[8] have been studied in clinical trials.

Monoamine oxidases (MAOs) are flavin adenine dinucleotide (FAD)-containing enzymes that are responsible for the oxidative deamination of neurotransmitters.[9] It is well known that high expression levels of MAO-B in neuronal tissue can increase the level of free radicals, which play a major role in the aetiology of AD.[10] Therefore, MAO inhibitors are considered potential candidates for anti-Alzheimer drugs because of their capacity to inhibit oxidative damage.[11] Among the MAO inhibitors, selegiline, which is an irreversible and selective MAO-B inhibitor, acts as a neuroprotective agent in cellular and animal models of AD.[12]

In recent years, the multi-target-directed ligand (MTDL) treatment strategy, which incorporates a sequential, multifactorial approach to a multifaceted disease such as AD, has been developed by many research groups.[13] For example, ladostigil (TV3326), the first anti-AD drug, targets cholinesterase, is a brain-selective MAO-B inhibitor, is neuroprotective,[14] and has been proven to be

* Corresponding authors. Tel./fax: +86 20 3994 3051 (L.H.), +86 20 3994 3050 (X.L.).
E-mail addresses: huangl72@mail.sysu.edu.cn (L. Huang), lixsh@mail.sysu.edu.cn (X. Li).

http://dx.doi.org/10.1016/j.bmc.2015.04.009
0968-0896/

safe and well tolerated in Phase I/IIa clinical trials and was taking part in Phase IIb in 2011 by Yissum, Pontifax, and Clal Biotechnology Industries. Previously, we reported the design, synthesis, and evaluation of a new series of tacrine–selegiline hybrids for the treatment of AD.[15] In this Letter, we report the study of the design, synthesis, and evaluation of a new series of hybrids that involves fusing important pharmacophores of selegiline and clioquinol in a new molecule.

2. Results and discussion

2.1. Chemistry

The synthetic route of the new selegiline derivatives is shown in Scheme 1. First, the commercially available 4-nitrophenyl acetic acid reacted with acetic anhydride and *N*-methylimidazole gave 4-nitrophenylacetone **2**.[16] **2** was hydrogenated in the presence of Pd/C, and the amino group was protected with di-*tert*-butyl dicarbonate to produce **3**, which reacted with (*R*)-1-phenylethanamine to provide chiral intermediate **4**.[17] Methylation and deprotection of **4** occurred in the presence of formaldehyde, H_2 and Pd/C to produce **5**. Compound **5** reacted with propargylbromide in the presence of potassium carbonate and subsequently with trifluoroacetic acid to produce **6**. Finally, compound **6** was reacted with 2-pyridinecarboxaldehyde derivatives or 2-hydroxybenzaldehyde derivatives to produce the target compounds **7** and **8**.

2.2. In vitro inhibition studies of hMAO-A and hMAO-B

The inhibitory activity of all target compounds against MAOs was determined with the recombinant human enzymes MAO-A and MAO-B using clorgyline and pargyline as the reference compounds (Table 1). As shown, most target compounds exhibit good activity against MAO-B with IC_{50} in the submicromolar range. Among them, compound **8a**, which has no substitutes other than hydroxyl on the A ring, gives the best result with an IC_{50} value of 0.21 μM. The substitutes at the R_1 or R_2 position seem to be unfavourable for the inhibition activities. Compounds **8b** and **8c**, which have methoxyl at the R_1 or R_2 position, have an IC_{50} value of more than 1 μM. Compounds **8d**, **8f** and **8i**, which have methoxyl, chlorine and hydroxyl at the R_2 position, have IC_{50} values of 0.31, 0.31 and 0.43 μM. When the A ring is replaced with pyridyl, compounds **7a** and **7b** also give good inhibition activities (**7a**: IC_{50} = 0.31 μM; **7b:** IC_{50} = 0.52 μM). The results in Table 1 indicate that some of the target compounds also possess effective MAO-A inhibition. In particular, **8d** (IC_{50} = 1.02 μM), **8f** (IC_{50} = 0.70 μM) and **8i** (IC_{50} = 1.03 μM) exhibit a good balance of inhibition for MAO-A and MAO-B. It is known that selective inhibitors for MAO-A have been used as effective anti-depressants,[18] and AD patients commonly present depressive symptoms, which implies that the dual inhibition of MAO-A and MAO-B can be beneficial to AD therapy.[19]

2.3. Molecular modelling studies of MAO-B

To evaluate the binding modes of the selegiline derivatives with MAO-B, docking simulation of compound **8a** were carried out using the CDOCKER program in the Discovery studio 2.1 software based on the X-ray crystal structure of human MAO-B (PDB entry 2V60). As shown in Figure 1, the Propargylamine group of selegiline moiety is properly oriented to the flavin adenine dinucleotide (FAD) cofactor adopting between Tyr394 (3.90 Å) and Tyr435 (5.51 Å) form face-to-face cation–π stacking interactions in a 'sandwich' form. Besides, the benzyl group embedded into a hydrophobic pocket delimited by Ile171, Cys172, Ile198, Ile199, Gln206, Tyr 326 and Phe343. Moreover, the OH atom of **8a** forms a direct hydrogen-bond contact with the backbone carbanyl group of Pro102 (average OH distance of 2.20 Å).

2.4. Anti-oxidant activity in vitro

To evaluate the antioxidant activities of selegiline derivatives, the oxygen radical absorbance capacity assay was performed using

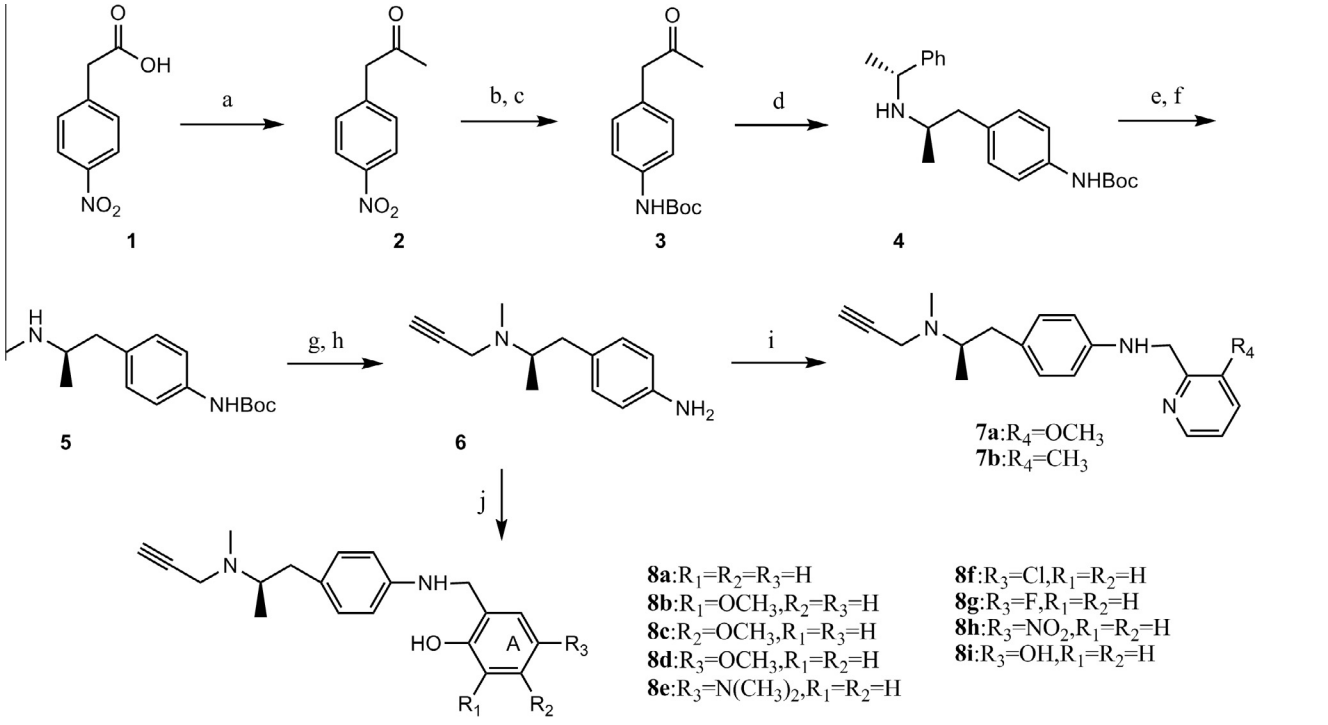

Scheme 1. Synthesis of target compounds. Reagents and conditions: (a) acetic anhydride, *N*-methylimidazole; (b) Pd/C, H_2, MeOH; (c) di-*tert*-butyl dicarbonate, Et_3N, CH_2Cl_2; (d) (i) (*R*)-1-phenylethanamine, Pt/C, H_2; (ii) L-(+)-tartaric acid, ethanol; (iii) NaOH, H_2O; (e) HCHO, Pt/C, MeOH; (f) Pd/C, H_2; (g) propargylbromide, K_2CO_3, MeCN, (h) trifluoroacetic acid, CH_2Cl_2; (i) different 2-pyridinecarboxaldehyde derivatives, rt; (j) different 2-hydroxybenzaldehyde derivatives, rt.

Please cite this article in press as: Xie, S.; et al. *Bioorg. Med. Chem.* (2015), http://dx.doi.org/10.1016/j.bmc.2015.04.009

Table 1
Inhibition of MAOs and oxygen radical absorbance capacity (ORAC, Trolox equivalents) of **7a**–**7b**, **8a**–**8i**, clorgyline, pargyline and selegiline

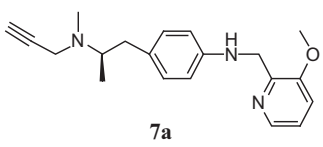

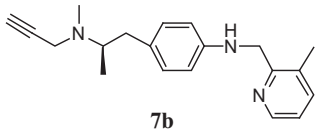

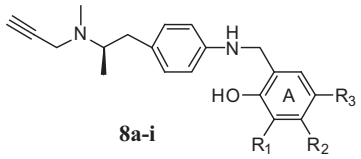

Compd	R	IC_{50} (μM) ± SD[a]		SI[b]	ORAC[c]
		MAO-A IC_{50}	MAO-B IC_{50}		
7a	—	3.41 ± 0.02	0.31 ± 0.03	11	1.49
7b	—	5.53 ± 0.04	0.52 ± 0.05	10.6	1.78
8a	$R_1 = R_2 = R_3 = H$	5.37 ± 0.03	0.21 ± 0.04	25.6	4.20
8b	$R_1 = OCH_3$, $R_2 = R_3 = H$	nt.	>1	—	2.44
8c	$R_2 = OCH_3$, $R_1 = R_3 = H$	nt.	>1	—	4.35
8d	$R_3 = OCH_3$, $R_1 = R_2 = H$	1.02 ± 0.05	0.31 ± 0.02	3.3	3.81
8e	$R_3 = N(CH_3)_2$, $R_1 = R_2 = H$	nt.	>1	—	4.52
8f	$R_3 = Cl$, $R_1 = R_2 = H$	0.70 ± 0.01	0.31 ± 0.06	2.2	4.44
8g	$R_3 = F$, $R_1 = R_2 = H$	nt.	>1	—	2.26
8h	$R_3 = NO_2$, $R_1 = R_2 = H$	nt.	0.95 ± 0.07	—	2.10
8i	$R_3 = OH$, $R_1 = R_2 = H$	1.03 ± 0.06	0.43 ± 0.02	2.4	5.67
Clorgyline	—	0.0041	nt.	—	nt.
Pargyline	—	nt.	0.1880	—	nt.
Selegiline	—	70.2 ± 3.8	0.0185 ± 0.002	37945	nt.

[a] Results are the mean of three independent experiments ($n = 3$) ± SD.
[b] Selectivity ratio: IC_{50}(MAO-A)/IC_{50}(MAO-B).
[c] The data are expressed as μ mol of Trolox equiv/μ mol tested compound.

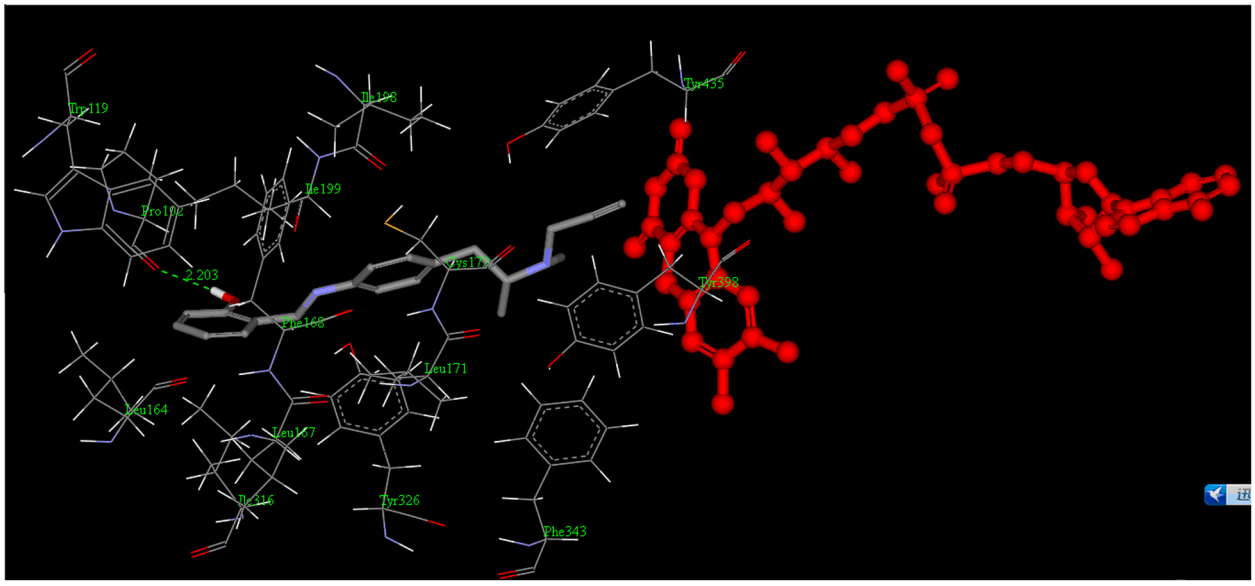

Figure 1. Docking pose of derivative **8a** into human MAO-B (2V60) highlighting the protein residues that establish the main interactions with **8a**. The FAD cofactor was depicted using ball and stick representation.

fluorescein (ORAC-FL),[20] and the vitamin E analogue Trolox was used as a standard. The results in Table 1 indicate that all target compounds exhibit excellent antioxidant capacity with ORAC-FL values of 1.49–5.65 Trolox equivalents. Compound **8i**, which features two hydroxyls in the A ring, exhibits the best result (5.67 Trolox equivalents). Generally, compounds 8**a**–**i** exhibit better activity (2.1–5.65 Trolox equivalents) than **7a**–**b** (1.49–1.78 Trolox equivalents), which demonstrates that pyridyl is unfavourable for antioxidant capacity.

2.5. Metal-chelating properties of compound 8a

The metal-chelating ability of the target compounds with **8a** as an example was investigated using UV–vis spectrometry.[21] The results in Figure 2 show that **8a** produces the maximum absorption peaks at 236 and 276 nm. After $CuSO_4$ was added to the solution of **8a**, the maximum absorption at 276 nm shifted to 282 nm, and the height of the peak at 236 nm obviously decreased, which demonstrates the formation of an **8a**–copper(II) complex. However, the

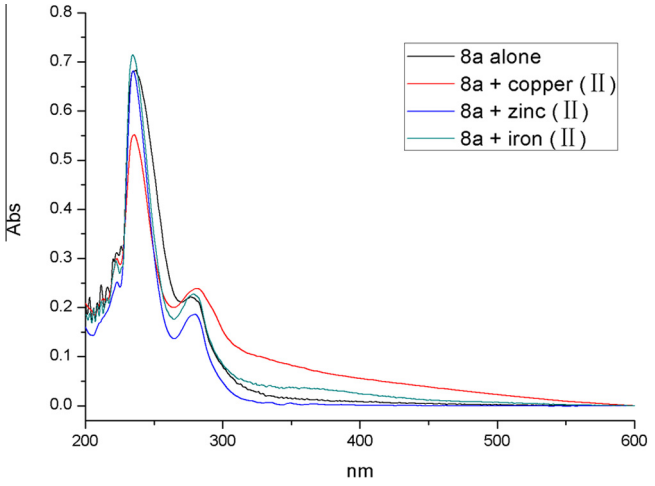

Figure 2. UV spectra of compound **8a** (40 μM) alone and in the presence of 20 μM $CuSO_4$, $FeSO_4$ or $ZnCl_2$. All solutions were prepared using a HEPES buffer solution (20 mM HEPES, 150 mM NaCl, pH 7.4).

specific absorbance at 236 nm and 276 nm slightly shifted when $FeSO_4$ or $ZnCl_2$ was mixed with **8a**, which suggests that **8a** can interact with iron(II) and zinc(II). To investigate the stoichiometry of the **8a**–Cu(II) complex, high-resolution mass spectrometry was performed (Fig. 3), and the peak of 675.6790, $[2M+Cu]^+$ determines that the stoichiometry of the **8a**–Cu(II) complex is 2:1.

2.6. Effects on Cu(II)-induced $A\beta_{1-42}$ aggregation using 8a, 8i, and 7a

To investigate the effects of the target compounds on metal-induced $A\beta_{1-42}$ aggregation, we used the ThT fluorescence binding assay to identify Cu(II)-induced $A\beta_{1-42}$ aggregation in the presence of **8a**, **8i** and **7a** with CQ as the reference.[8] As shown in Figure 4, the fluorescence of $A\beta_{1-42}$ treated with Cu(II) is 143% of that of $A\beta_{1-42}$ alone, which indicates that $A\beta_{1-42}$ aggregation is indeed accelerated by Cu(II). In contrast, the fluorescence values of $A\beta_{1-42}$ treated with Cu(II) and **8a**, **8i**, and **7a** and CQ are obviously lower than that of $A\beta_{1-42}$ alone ($A\beta_{1-42}$ alone: 100%; **8a**: 69.10%; **8i**: 40.37%; **7a**: 63.09%; CQ: 68.25%), which suggests that our target compounds can effectively inhibit the Cu(II)-induced $A\beta_{1-42}$ aggregation.

2.7. In vitro blood–brain barrier permeation assay

The ability to cross the blood–brain barrier (BBB) and reach their therapeutic targets is important for CNS drugs. To evaluate

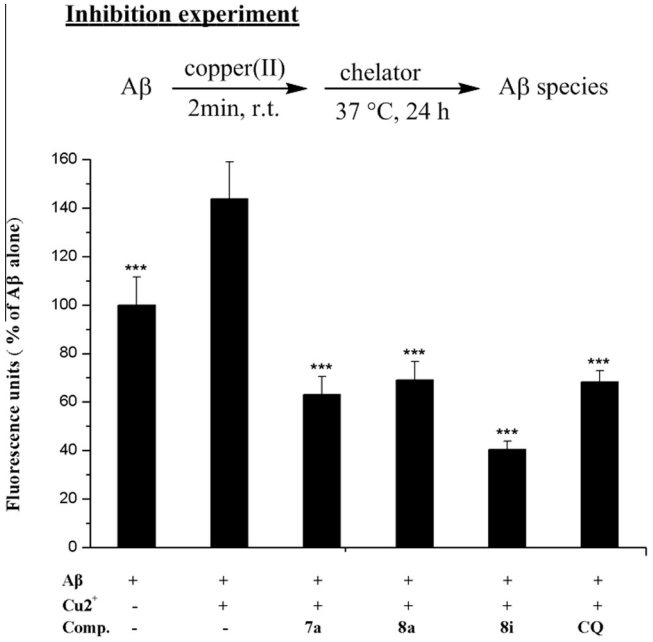

Figure 4. The inhibition of copper(II)-induced $A\beta_{1-42}$ aggregation by **7a**, **8a**, **8i** and CQ ($[A\beta_{1-42}]$ = copper(II) = 25 μM, [**7a**] = [**8a**] = [**8i**] = [CQ] = 50 μM, 37 °C, 24 h). Top: Scheme of the inhibition experiment. Bottom: Results of the ThT binding assay. Statistical comparisons with control ($A\beta_{1-42}$ aggregation in the presence of copper(II)) were performed by a one-way ANOVA followed by Dunnett's multiple comparison test using Graph Pad Prism 5.0 Software (level of significance $^{***}p$ <0.001).

the brain penetration of the target compounds, the parallel artificial membrane permeation assay for the blood brain barrier (PAMPA–BBB), which was described by Di et al.[22] and successfully applied by some of us to different classes of compounds. First, we compared the permeability of 13 commercial drugs with reported values to validate the assay. A plot of the experimental data versus the reported values produced a good linear correlation: P_e (exp.) = 1.4574P_e (bibil.) − 1.0773 (R^2 = 0.9427). From this equation and considering the limit established by Di et al. for blood–brain barrier permeation, we found that molecules with a permeability above 4.7×10^{-6} cm s^{-1} would be able to cross the BBB by passive permeation (CNS+). P_e values from 1.8×10^{-6} cm s^{-1} to 4.7×10^{-6} cm s^{-1} were classified as 'CNS+/−' (BBB permeation uncertain). The results of the PAMPA–BBB assay of the tested compounds are presented in Table 2, which indicated that **8a**, **8d**, **8e**, **7a** and **7b** can cross the BBB, whereas the status of **8i** is uncertain.

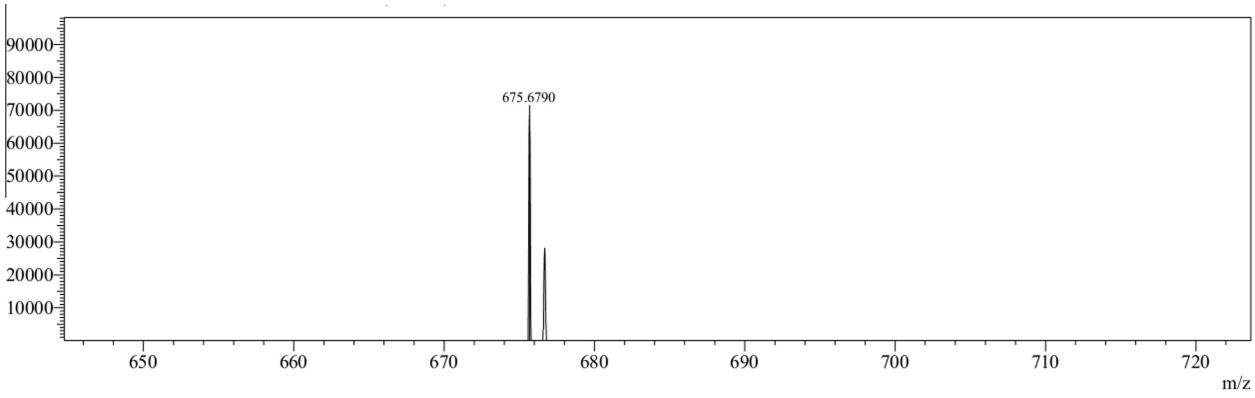

Figure 3. HRMS spectrum of **8a**–Cu(II) complex.

Table 2
Permeability ($P_e \times 10^{-6}$ cm s^{-1}) in the PAMPA-BBB assay for the selected compounds and their predicted penetration into the CNS

Compd[a]	P_e ($\times 10^{-6}$ cm s^{-1})[b]	Prediction
7a	12.8 ± 0.7	CNS+
7b	12.1 ± 0.8	CNS+
8a	11.5 ± 0.5	CNS+
8d	11.7 ± 0.5	CNS+
8e	12.5 ± 1.0	CNS+
8i	3.1 ± 0.3	CNS+/−

[a] Compounds were dissolved in DMSO at 5 mg/mL and diluted with PBS/EtOH (70:30). The final concentration of compounds was 100 μg/mL.
[b] Values are expressed as the mean ± SD of three independent experiments.

3. Conclusion

In summary, we have developed a series of compounds by merging the main pharmacophores of the MAO inhibitor selegiline and biometal chelator clioquinol to treat Alzheimer's disease. The in vitro assays show that these compounds have both MAO-B inhibition activities, antioxidant activity and biometal chelating ability, which can effectively inhibit Cu(II)-induced $A\beta_{1-42}$ aggregation. Among the compounds, compound **8a** exhibits good inhibitory potency toward MAO-B (IC_{50} = 0.21 μM) and good antioxidant activity (ORAC = 4.20). The parallel artificial membrane permeation assay shows that most target compounds can cross the BBB. These results indicate that compound **8a** may be a good multifunctional agent for the treatment of AD. Further studies based on these results are in progress.

4. Experimental

4.1. Chemistry

The ^{1}H NMR and ^{13}C NMR spectra were collected on a Bruker BioSpin GmbH spectrometer at 400 MHz with TMS as the internal standard. The high-resolution mass spectra were obtained using a Shimadzu LCMS-IT-TOF mass spectrometer. High-performance liquid chromatography (HPLC), which was equipped with a TC-C18 column (4.6 × 250 mm, 5 μm), was used to determine the purity of the synthesised compounds.

4.2. Synthesis procedure of intermediates 2-6

4.2.1. Synthesis procedure of 1-(4-nitrophenyl)propan-2-one (2)

In a stirred solution of 4-nitrophenyl acetic acid (0.05 mol, 1 equiv) in acetic anhydride (25 mL, 5 equiv), *N*-methylimidazole (0.025 mol, 0.5 equiv) was added at room temperature. After stirring for 6 h in nitrogen atmosphere, the reaction was quenched by adding water (20 mL). The mixture was extracted (EtOAc), washed ($NaHCO_3$ and subsequently with H_2O), dried (Na_2SO_4), filtered and concentrated to give the product as a yellow solid (yield: 70%). ^{1}H NMR (400 MHz, $CDCl_3$): δ 8.18 (d, J = 8.4 Hz, 2H), 7.35 (d, J = 8.4 Hz, 2H), 3.84 (s, 2H), 2.23 (s, 3H).

4.2.2. Synthesis procedure of *tert*-butyl(4-(2-oxopropyl) phenyl)carbamate (3)

(b) To a solution of **2** (4.0 mmol) in MeOH (20.0 mL), Pd/C (5% m/m) was added, and the reaction mixture was charged with H_2 atmosphere. After the resulting solution was stirred at room temperature for 4 h, the mixture was filtered and concentrated to produce a light yellow solid. (c) The yellow solid was dissolved in 25.0 mL of a THF and H_2O mixture (1:1). After potassium carbonate (4.0 mmol) was added to the mixture and stirred for 5 min, di-*tert*-butyl dicarbonate (6.0 mmol) was added. After the reaction mixture was stirred for 10 h, the organic phases were separated, and the aqueous phase was extracted (EtOAc). The combined organic layers were washed (brine), dried (Na_2SO_4), filtered, and concentrated. The residue was purified using silica gel column chromatography (PE/EA = 10) to produce compound **3** as a white solid (75% yield). ^{1}H NMR (400 MHz, $CDCl_3$) δ 7.32 (d, J = 8.4 Hz, 1H), 7.11 (d, J = 8.5 Hz, 1H), 6.59 (s, 1H), 3.62 (s, 1H), 2.12 (s, 1H), 1.50 (s, 4H).

4.2.3. Synthesis procedure of *tert*-butyl(4-((*R*)-2-(((*R*)-1-phenylethyl)amino)propyl)phenyl)carbamate (4)

To a solution of **3** (3.0 mmol) and (*R*)-1-phenylethanamine (3.0 mmol) in MeOH (10.0 mL), Pt/C (5% m/m) was added, and the reaction mixture was charged with H_2 atmosphere (20 bar). After the solution was stirred at room temperature for 24 h, the reaction mixture was filtered and concentrated. The residue was purified using silica gel column chromatography to produce **4** as a light yellow oil (90% yield). ^{1}H NMR (400 MHz, $CDCl_3$) δ 7.37–7.25 (m, 4H), 7.19 (d, J = 8.4 Hz, 3H), 6.93 (d, J = 8.4 Hz, 2H), 6.37 (s, 1H), 3.64–3.69 (m, 1H), 2.97–3.02 (m, 1H), 2.85 (dd, J = 13.1, 4.7 Hz, 1H), 2.30 (dd, J = 13.1, 9.3 Hz, 1H), 1.50 (s, 9H), 1.30 (d, J = 6.6 Hz, 3H), 0.87 (d, J = 6.6 Hz, 3H).

4.2.4. Synthesis procedure of (*R*)-*tert*-butyl(4-(2-(methylamino)propyl)phenyl)carbamate (5)

Pt (10% m/m) was slowly added to a mixture of compound **4** (5.0 mmol), formalin (3.0 mL) and methanol (15 mL), and the reaction mixture was charged with H_2 atmosphere. After the mixture was stirred for 12 h, the catalyst was filtered away, and the filtrate was evaporated in vacuum to produce a colourless oil. (f) To a solution of that oil (5.0 mmol) in methanol (10 mL), 10% Pd/C was added, and the mixture was stirred in a hydrogen atmosphere (1.5 MPa pressure) at 40 °C for 24 h. After the reaction was completed, the catalyst was filtered away, and the filtrate was evaporated to produce **5** as a white oil (yield: 80%). ^{1}H NMR (400 MHz, $CDCl_3$) δ 7.41–7.20 (m, 2H), 7.11 (d, J = 8.4 Hz, 2H), 2.88–2.66 (m, 2H), 2.60 (dd, J = 13.2, 6.5 Hz, 1H), 2.41 (s, 3H), 1.51 (s, 9H), 1.07 (d, J = 6.2 Hz, 3H).

4.2.5. Synthesis procedure of (*R*)-4-(2-(methyl(prop-2-yn-1-yl)amino)propyl)aniline (6)

(g) To a solution of **5** (3 mmol) and potassium carbonate (4.5 mmol) in acetonitrile (20.0 mL), propargylbromide (80% in toluene, 3 mmol) was slowly added. After the reaction mixture was stirred in nitrogen atmosphere at room temperature for 12 h, the reaction mixture was filtered and concentrated to produce a colourless oil (65% yield). (h) Trifluoroacetic acid was slowly added to a solution of that oil (3 mmol) in dichloromethane (15 mL) at 0 °C; then, the mixture was stirred at room temperature for 8 h. After the solvent was evaporated in vacuum, the residue was purified using silica gel column chromatography to produce compound **6** as a colourless oil (90% yield). ^{1}H NMR (400 MHz, $CDCl_3$) δ 6.95 (d, J = 8.3 Hz, 2H), 6.67–6.49 (m, 2H), 3.41 (d, J = 1.6 Hz, 2H), 2.94–2.85 (m, 2H), 2.40 (s, 3H), 2.32–2.24 (m, 1H), 2.23 (s, 1H), 0.95 (d, J = 6.8 Hz, 3H).

4.3. General synthesis procedure of 7a–b and 8a–i

To a solution of compound **6** (1 mmol) in ethanol (5 mL), aldehyde (1 mmol) was added, and the resulting mixture was stirred at room temperature. After the substrates disappeared (monitored using TLC), $NaBH_4$ (3 mmol) was gradually added at 0 °C. After the mixture was stirred for 1 h, water (10 mL) was added, and the mixture was extracted using ethyl acetate. The organic phases were evaporated in vacuum, and the residue was purified using silica gel column chromatography to produce the compounds.

4.3.1. (*R*)-*N*-((3-Methoxypyridin-2-yl)methyl)-4-(2-(methyl(prop-2-yn-1-yl)amino)propyl)aniline (7a)

6-Methoxypyridine-2-carbaldehyde was treated with **7** according to the general procedure to give the desired product **7a** as an oil (82% yield). IR: 3427, 3308, 2950, 2922, 1311, 1262, 794, 732 cm^{-1}; ^1H NMR (400 MHz, $CDCl_3$) δ 7.51 (dd, J = 8.1, 7.4 Hz, 1H), 6.99 (d, J = 8.4 Hz, 2H), 6.89 (d, J = 7.3 Hz, 1H), 6.62 (dd, J = 8.6, 2.5 Hz, 3H), 4.33 (s, 2H), 3.95 (s, 3H), 3.41 (d, J = 1.6 Hz, 2H), 2.98–2.84 (m, 2H), 2.41 (s, 3H), 2.28 (dd, J = 12.6, 9.4 Hz, 1H), 2.23 (t, J = 2.4 Hz, 1H), 0.96 (d, J = 6.7 Hz, 3H). ^{13}C NMR (101 MHz, $CDCl_3$) δ 163.84, 156.32, 146.32, 139.07, 130.01, 129.18, 114.06, 113.21, 108.75, 80.52, 72.43, 59.68, 53.32, 49.32, 43.13, 38.91, 37.52, 15.03. HRMS calcd for $[M+H]^+$: 324.2070; found: 324.2069; HPLC purity: 97.6%.

4.3.2. (*R*)-4-(2-(Methyl(prop-2-yn-1-yl)amino)propyl)-*N*-((3-methylpyridin-2-yl)methyl)aniline (7b)

6-Methyl-2-pyridinecarboxaldehyde was treated with **7** according to the general procedure to give the desired product **7b** as an oil (76% yield). IR: 3392, 3297, 2961, 2924, 2100, 1316, 1259, 781, cm^{-1}; ^1H NMR (400 MHz, $CDCl_3$) δ 7.51 (t, J = 7.7 Hz, 1H), 7.13 (d, J = 7.7 Hz, 1H), 7.02 (d, J = 7.6 Hz, 1H), 6.98 (d, J = 8.4 Hz, 2H), 6.60 (d, J = 8.5 Hz, 2H), 4.39 (s, 2H), 3.41 (d, J = 1.9 Hz, 2H), 3.01–2.79 (m, 2H), 2.56 (s, 3H), 2.40 (s, 3H), 2.32–2.25 (m, 1H), 2.22 (t, J = 2.4 Hz, 1H), 0.95 (d, J = 6.7 Hz, 3H). ^{13}C NMR (101 MHz, $CDCl_3$) δ 158.01, 157.97, 146.25, 136.81, 129.99, 129.10, 121.54, 118.45, 113.11, 80.55, 72.38, 59.68, 49.65, 43.13, 38.92, 37.51, 24.43, 15.05. HRMS calcd for $[M+H]^+$: 308.2121; found: 308.2115; HPLC purity: 99.4%.

4.3.3. (*R*)-2-(((4-(2-(Methyl(prop-2-yn-1-yl)amino)propyl)phenyl)amino)methyl)phenol (8a)

2-Hydroxybenzaldehyde was treated with **7** according to the general procedure to give the desired product **8a** as a light yellow oil (80% yield). IR: 3515, 3424, 3316, 2963, 2920, 2106, 1301, 1277, 1239, 758 cm^{-1}; ^1H NMR (400 MHz, $CDCl_3$) δ 7.25–7.18 (m, 1H), 7.18–7.12 (m, 1H), 7.05 (d, J = 8.4 Hz, 2H), 6.87 (m, 2H), 6.83–6.72 (m, 2H), 4.40 (s, 2H), 3.42 (d, J = 1.4 Hz, 2H), 3.01–2.86 (m, 2H), 2.41 (s, 3H), 2.37–2.28 (m, 1H), 2.24 (s, 1H), 0.96 (d, J = 6.7 Hz, 3H). ^{13}C NMR (101 MHz, $CDCl_3$) δ 156.91, 145.25, 132.68, 130.12, 129.16, 128.64, 123.00, 119.96, 116.64, 116.02, 80.42, 72.49, 59.46, 49.08, 43.15, 39.01, 37.46, 15.00. HRMS calcd for $[M-H]^-$: 307.1816; found: 307.1816; purity: 96.8%.

4.3.4. (*R*)-2-Methoxy-6-(((4-(2-(methyl(prop-2-yn-1-yl)amino)propyl)phenyl)amino)methyl)phenol (8b)

2-Hydroxy-3-methoxybenzaldehyde was treated with **7** according to the general procedure to give the desired product **8b** as an oil (75% yield). IR: 3516, 3392, 3303, 2967, 2920, 2107, 1265, 1217, 1188, 735 cm^{-1}; ^1H NMR (400 MHz, $CDCl_3$) δ 6.99 (d, J = 8.4 Hz, 2H), 6.89 (p, J = 4.0 Hz, 1H), 6.83–6.77 (m, 2H), 6.65 (d, J = 8.5 Hz, 2H), 4.36 (s, 2H), 3.88 (s, 3H), 3.42 (d, J = 1.9 Hz, 2H), 2.98–2.83 (m, 2H), 2.41 (s, 3H), 2.28 (d, J = 3.2 Hz, 1H), 2.23 (t, J = 2.4 Hz, 1H), 0.96 (d, J = 6.7 Hz, 3H). ^{13}C NMR (101 MHz, $CDCl_3$) δ 146.91, 146.25, 144.33, 129.98, 129.94, 124.81, 121.17, 119.54, 113.94, 110.08, 80.52, 72.46, 59.66, 56.04, 44.78, 43.13, 38.93, 37.52, 15.04. HRMS calcd for $[M+H]^+$: 339.2067; found: 339.2082; HPLC purity: 96.5%.

4.3.5. (*R*)-5-Methoxy-2-(((4-(2-(methyl(prop-2-yn-1-yl)amino)propyl)phenyl)amino)methyl)phenol (8c)

2-Hydroxy-4-methoxybenzaldehyde was treated with **7** according to the general procedure to give the desired product **8c** as an oil (82%yield). IR: 3396, 3305, 3264, 2960, 2926, 2116, 1323, 1283, 758, 712 cm^{-1}; ^1H NMR (400 MHz, $CDCl_3$) δ 7.04 (dd, J = 10.3, 8.4 Hz, 3H), 6.87–6.74 (m, 2H), 6.47 (d, J = 2.5 Hz, 1H), 6.43 (dd, J = 8.3, 2.5 Hz, 1H), 4.34 (s, 2H), 3.78 (s, 3H), 3.41 (s, 2H), 3.03–2.83 (m, 2H), 2.41 (s, 3H), 2.37–2.27 (m, 1H), 2.23 (t, J = 2.4 Hz, 1H), 0.96 (d, J = 6.7 Hz, 3H). ^{13}C NMR (101 MHz, $CDCl_3$) δ 160.72, 158.01, 145.29, 132.68, 130.10, 129.21, 116.10, 115.23, 105.87, 102.23, 80.42, 72.50, 59.47, 55.31, 48.62, 43.15, 39.00, 37.47, 14.99. HRMS calcd for $[M-H]^-$: 337.1922; found: 337.1926; HPLC purity: 98.8%.

4.3.6. (*R*)-4-Methoxy-2-(((4-(2-(methyl(prop-2-yn-1-yl)amino)propyl)phenyl)amino)methyl)phenol (8d)

2-Hydroxy-5-methoxybenzaldehyde was treated with **7** according to the general procedure to give the desired product **8d** as an oil (73% yield). IR: 3411, 3288, 3228, 2952, 2930, 2121, 1267, 1201, 806, 736 cm^{-1}; ^1H NMR (400 MHz, $CDCl_3$) δ 7.09–6.98 (m, 2H), 6.78 (m, 5H), 4.34 (s, 2H), 3.76 (t, J = 1.7 Hz, 3H), 3.41 (s, 2H), 2.99–2.85 (m, 2H), 2.40 (d, J = 1.5 Hz, 3H), 2.31 (td, J = 11.0, 5.6 Hz, 1H), 2.24 (t, J = 2.1 Hz, 1H), 0.96 (d, J = 6.7 Hz, 3H). ^{13}C NMR (101 MHz, $CDCl_3$) δ 153.08, 150.58, 145.36, 132.40, 130.11, 123.90, 117.10, 115.82, 114.40, 113.93, 80.34, 72.60, 59.48, 55.81, 48.95, 43.14, 38.95, 37.48, 14.98. HRMS calcd for $[M-H]^-$: 337.1922; found: 337.1919; HPLC purity: 96.2%.

4.3.7. (*R*)-4-(Dimethylamino)-2-(((4-(2-(methyl(prop-2-yn-1-yl)amino)propyl)phenyl)amino)methyl)phenol (8e)

5-(Dimethylamino)-2-hydroxybenzaldehyde was treated with **7** according to the general procedure to give the desired product **8e** as an oil (79% yield). IR: 3394, 3273, 3191, 2957, 2922, 2111, 1248, 1189, 807, 757 cm^{-1}; ^1H NMR (400 MHz, $CDCl_3$) δ 7.04 (d, J = 8.4 Hz, 2H), 6.81 (d, J = 8.7 Hz, 1H), 6.77 (t, J = 5.5 Hz, 2H), 6.69 (d, J = 8.5 Hz, 1H), 6.63 (s, 1H), 4.34 (s, 2H), 3.42 (s, 2H), 3.00–2.89 (m, 2H), 2.86 (s, 6H), 2.41 (s, 3H), 2.36–2.27 (m, 1H), 2.24 (t, J = 2.4 Hz, 1H), 0.96 (d, J = 6.7 Hz, 3H). ^{13}C NMR (101 MHz, $CDCl_3$) δ 148.71, 145.59, 145.23, 132.18, 130.08, 123.57, 117.07, 115.72, 114.76, 114.55, 80.41, 72.55, 59.51, 49.23, 43.15, 41.96, 38.97, 37.49, 15.01. HRMS calcd for $[M-H]^-$: 350.2238; found: 350.2242; HPLC purity: 97.6%.

4.3.8. (*R*)-4-Chloro-2-(((4-(2-(methyl(prop-2-yn-1-yl)amino)propyl)phenyl)amino)methyl)phenol (8f)

5-Chloro-2-hydroxybenzaldehyde was treated with 7 according to the general procedure to give the desired product **8f** as an oil (83% yield). IR: 3445, 3294, 2968, 2925, 2122, 1270, 1251, 814, 736 cm^{-1}; ^1H NMR (400 MHz, $CDCl_3$) δ 7.14 (dt, J = 7.3, 2.4 Hz, 2H), 7.05 (d, J = 8.4 Hz, 2H), 6.79 (d, J = 8.4 Hz, 1H), 6.75 (d, J = 8.4 Hz, 2H), 4.35 (s, 2H), 3.41 (s, 2H), 2.99–2.86 (m, 2H), 2.40 (s, 3H), 2.37–2.28 (m, 1H), 2.24 (t, J = 2.4 Hz, 1H), 0.96 (d, J = 6.6 Hz, 3H). ^{13}C NMR (101 MHz, $CDCl_3$) δ 155.54, 144.94, 132.79, 130.18, 128.78, 128.21, 124.65, 124.46, 117.91, 116.02, 80.25, 72.69, 59.44, 48.65, 43.13, 38.92, 37.44, 14.93. HRMS calcd for $[M-H]^-$: 341.1426; found: 341.1434; HPLC purity: 98.5%.

4.3.9. (*R*)-4-Fluoro-2-(((4-(2-(methyl(prop-2-yn-1-yl)amino)propyl)phenyl)amino)methyl)phenol (8g)

5-Fluoro-2-hydroxybenzaldehyde was treated with **7** according to the general procedure to give the desired product **8g** as an oil (85%yield). IR: 3345, 3295, 3137, 2966, 2929, 2103, 1286, 1248, 819, 722 cm^{-1}; ^1H NMR (400 MHz, $CDCl_3$) δ 7.05 (d, J = 8.4 Hz, 2H), 6.94–6.83 (m, 2H), 6.83–6.78 (m, 1H), 6.76 (d, J = 8.5 Hz, 2H), 4.36 (d, J = 3.2 Hz, 2H), 3.41 (s, 2H), 2.99–2.85 (m, 2H), 2.40 (s, 3H), 2.37–2.27 (m, 1H), 2.23 (t, J = 2.4 Hz, 1H), 0.96 (d, J = 6.7 Hz, 3H). ^{13}C NMR (101 MHz, CDCl3) δ 156.44 (d, J = 237.6 Hz), 152.83 (d, J = 2.1 Hz), 144.95, 132.91, 130.17, 124.02 (d, J = 6.7 Hz), 117.39 (d, J = 7.9 Hz), 116.02, 115.08 (d, J = 59.59 Hz), 115.08 (d, J = 13.8 Hz), 80.38, 72.53, 59.44, 48.86, 43.15, 38.99, 37.46, 14.97. HRMS calcd for $[M+H]^+$: 327.1867; found: 327.1873; HPLC purity: 95.8%.

Please cite this article in press as: Xie, S.; et al. *Bioorg. Med. Chem.* (2015), http://dx.doi.org/10.1016/j.bmc.2015.04.009

4.3.10. (*R*)-2-(((4-(2-(Methyl(prop-2-yn-1-yl)amino)propyl) phenyl)amino)methyl)-4-nitrophenol (8h)

2-Hydroxy-5-nitrobenzaldehyde was treated with 7 according to the general procedure to give the desired product **8h** as an oil (86% yield). IR: 3240, 3286, 2968, 2923, 2128, 1334, 1285 828, 752 cm^{-1}; ^1H NMR (400 MHz, $CDCl_3$) δ 8.16–8.03 (m, 2H), 7.05 (d, J = 8.4 Hz, 2H), 6.90–6.83 (m, 1H), 6.75 (d, J = 8.4 Hz, 2H), 4.47 (s, 2H), 3.48 (s, 2H), 2.98–2.85 (m, 2H), 2.40 (s, 3H), 2.37–2.27 (m, 1H), 2.23 (t, J = 2.4 Hz, 1H), 0.95 (d, J = 6.6 Hz, 3H). ^{13}C NMR (101 MHz, $CDCl_3$) δ 163.60, 144.41, 139.20, 133.28, 130.26, 125.32, 124.60, 123.69, 116.90, 116.18, 80.24, 72.63, 59.38, 48.61, 43.12, 38.97, 37.40, 14.88. HRMS calcd for $[M-H]^-$: 352.1667; found: 352.1661; HPLC purity: 97.2%.

4.3.11. (*R*)-2-(((4-(2-(Methyl(prop-2-yn-1-yl)amino)propyl) phenyl)amino)methyl)benzene-1,4-diol (8i)

2,5-Dihydroxybenzaldehyde was treated with **7** according to the general procedure to give the desired product **8i** as an oil (77% yield). IR: 3408, 3281, 2961, 2924, 2120, 1264, 1199, 811, 729 cm^{-1}; ^1H NMR (400 MHz, $CDCl_3$) δ 7.00 (d, J = 8.4 Hz, 2H), 6.72 (d, J = 8.4 Hz, 3H), 6.69–6.62 (m, 2H), 4.27 (s, 2H), 3.42 (s, 2H), 2.93 (tt, J = 10.7, 5.2 Hz, 2H), 2.41 (s, 3H), 2.31 (dd, J = 14.0, 10.7 Hz, 1H), 2.25 (t, J = 2.4 Hz, 1H), 0.96 (d, J = 6.4 Hz, 3H). ^{13}C NMR (101 MHz, $CDCl_3$) δ 150.04, 149.22, 145.43, 132.06, 130.10, 124.10, 117.19, 115.77, 115.63, 79.93, 72.99, 59.49, 48.57, 43.08, 38.85, 37.44, 14.79. HRMS calcd for $[M-H]^-$: 323.1765; found: 323.1770; HPLC purity: 98.3%.

4.4. Biological assays

4.4.1. In vitro inhibition of monoamine oxidase

Recombinant hMAO-A and hMAO-B from Sigma–Aldrich were adjusted to 12.5 μg/mL and 75 μg/mL, respectively, of the test compound, and 80 μL of MAO was incubated for 15 min at 37 °C in a flat, black-bottomed 96-well microtest plate in the dark. Amplex Red reagent (200 μM), horseradish peroxidase (2 U/mL), and *p*-tyramine (2 mM) for hMAO-A or benzylamine (2 mM) for hMAO-B were added to start the reaction. After 20 min of incubation at 37 °C, the assay was quantified in a multidetection microplate fluorescence reader based on the generated fluorescence (excitation, 545 nm; emission, 590 nm). The specific fluorescence emission was calculated after subtracting the background activity, which was determined from vials that contained all components except the hMAO isoforms, which were replaced by a sodium phosphate buffer solution.

4.4.2. Docking study

The simulation system was built based on the structure obtained from the Protein Data Bank (PDB: 2V60 for MAO-B). The heteroatoms and water molecules were removed, and all hydrogen atoms were subsequently added to the protein. Then force field was assigned to the enzyme. The ligand binding site was defined as 13 Å from the original ligand. Prior to the docking calculations, the original ligand was removed. The 3D structures of compound **10** were generated and optimised with the Discovery Studio 2.1 package (Accelrys Inc., San Diego, CA).

The CDOCKER program of the Discovery Studio 2.1 software, which allows full flexibility of ligands, was used to perform docking simulations. The docking and subsequent scoring were performed using the default parameters of the CDOCKER program. CDOCKER_INTERACTION_ENERGY is used like a score where a lower value indicates a more favourable binding.

4.4.3. ThT assay

$A\beta_{1-42}$ (Millipore, counter ion: NaOH) was dissolved in a solution of ammonium hydroxide (1%) to produce a stock solution (2000 μM), which was aliquoted into small samples and stored at −80 °C. For the copper-induced $A\beta_{1-42}$ aggregation experiment, the stock solution was diluted with 20 μM HEPES (pH = 6.6), 150 μM NaCl. Inhibition aggregation experiment: a mixture of the peptide with or without copper and tested compound was incubated at 37 °C for 24 h and subsequently diluted to a final volume of 200 μL with 50 mM glycine–NaOH buffer (pH 8.0), which contained thioflavin T (5 μM). A 300-s time scan of fluorescence intensity was performed (λ_{exc} = 450 nm; λ_{em} = 485 nm), and values at the plateau were averaged after subtracting the background fluorescence of thioflavin T solution.

4.4.4. Oxygen radical absorbance capacity (ORAC-FL) assay

The fluorescein (FL) stock solution and the tested compound were diluted with phosphate buffer (75 mM, pH 7.4) to 0.117 μM and 20 μM, respectively. The solution of (±)-6-hydroxy-2,5,7,8-tetramethylchroman-2-carboxylic acid (Trolox) was diluted with the same buffer to 100, 80, 60, 50, 40, 20, and 10 μM. The solution of 2,2′-azobis-(amidinopropane) dihydrochloride (AAPH) was prepared before the experiment by dissolving 108.4 mg AAPH in 10 mL 75 mM phosphate buffer (pH 7.4) to 40 mM. The mixture of the tested compound (20 μL) and FL (120 μL; 70 nM, final concentration) was pre-incubated for 10 min at 37 °C; then, 60 μL of the AAPH solution was added. The fluorescence was recorded every minute for 120 min (λ_{exc} = 485 nm; λ_{em} = 520 nm). The fluorescence measurements were normalised to the curve of the blank (without antioxidant). The ORAC-FL values were calculated as previously described.

4.4.5. Metal-chelating study

The chelating studies were performed using a UV–vis spectrophotometer. The absorption spectra of each compound, alone or in the presence of $CuSO_4$, $FeSO_4$ or $ZnCl_2$ for 30 min, were recorded at room temperature. The stoichiometry of the complex compound-Cu^{2+} was determined using high-resolution mass spectrometry. From separate solutions of the compound and $CuSO_4$, the solutions were obtained if the sum of the concentrations of both species was constant in all samples but the proportions of both components varied between 0% and 100%.

4.4.6. In vitro blood–brain barrier permeation assay

The brain penetration of the compounds was evaluated using a parallel artificial membrane permeation assay (PAMPA), which was described by Di et al. Commercial drugs were purchased from Sigma and Alfa Aesar. The porcine brain lipid (PBL) was obtained from Avanti Polar Lipids. The donor microplate (PVDF membrane, pore size 0.45 mm) and the acceptor microplate were obtained from Millipore. The 96-well UV plate (COSTAR®) was obtained from Corning Incorporated. The acceptor 96-well microplate was filled with 300 μL of PBS/EtOH (7:3), and the filter membrane was impregnated with 4 μL of PBL in dodecane (20 mg mL^{-1}). The compounds were dissolved in DMSO at 5 mg mL^{-1} and diluted 50-fold in PBS/EtOH (7:3) to obtain a concentration of 100 mg mL^{-1}; then, 200 μL was added to the donor wells. The acceptor filter plate was carefully put on the donor plate to form a sandwich, which was left undisturbed for 10 h at 25 °C. After incubation, the donor plate was carefully removed, and the concentrations of the compounds in the acceptor wells were determined using the UV plate reader (Flexstation® 3). Every sample was analysed at five wavelengths, in four wells, and in at least three independent runs, and the results are given as the mean ± standard deviation. In each experiment, 13 quality control standards with known BBB permeability were included to validate the analysis set. A plot of experimental data versus bibliographic values gives a good linear correlation: P_e (exp.) = 1.4574P_e (bibil.) − 1.0773 (R^2 = 0.9427). Based on this equation and

considering the limit established by Di et al. for blood–brain barrier permeation, we found that the compounds with permeability above 4.7×10^{-6} cm s^{-1} could cross the blood–brain barrier.

Acknowledgments

We thank the Natural Science Foundation of China (No. 21302235), Guangdong Natural Science Foundation (2014A030313124) and the Ph.D. Programs Foundation of the Ministry of Education of China (20120171120045) for financial support of this study.

References and notes

1. (a) Rook, Y.; Schmidtke, K. U.; Gaube, F.; Schepmann, D.; Wunsch, B.; Heilmann, J.; Lehmann, J.; Winckler, T. *J. Med. Chem.* **2010**, *53*(9), 3611; (b) Björklund, C.; Oscarson, S.; Benkestock, K.; Borkakoti, N.; Jansson, K.; Lindberg, J.; Vrang, L.; Hallberg, A.; Rosenquist, Å.; Samuelsson, B. *J. Med. Chem.* **2010**, *53*(4), 1458.
2. Van der Zee, E. A.; Platt, B.; Riedel, G. *Behav. Brain. Res* **2011**, *221*(2), 583.
3. Scarpini, E.; Schelterns, P.; Feldman, H. *Lancet Neurol.* **2003**, *2*(9), 539.
4. Cavalli, A.; Bolognesi, M. L.; Minarini, A.; Rosini, M.; Tumiatti, V.; Recanatini, M.; Melchiorre, C. *J. Med. Chem.* **2008**, *51*(3), 347.
5. (a) Barnham, K. J.; Bush, A. I. *Chem. Soc. Rev.* **2014**, *43*(19), 6727; (b) Hayne, D. J.; Lim, S.; Donnelly, P. S. *Chem. Soc. Rev.* **2014**, *43*(19), 6701.
6. Lovell, M. A.; Robertson, J. D.; Teesdale, W. J.; Campbell, J. L.; Markesbery, W. R. *J. Neurol. Sci.* **1998**, *158*(1), 47.
7. Dong, J.; Atwood, C. S.; Anderson, V. E.; Siedlak, S. L.; Smith, M. A.; Perry, G.; Carey, P. R. *Biochemistry* **2003**, *42*(10), 2768.
8. Ritchie, C. W.; Bush, A. I.; Mackinnon, A., et al. *Arch. Neurol.-Chicago* **2003**, *60*(12), 1685.
9. Chaurasiya, N. D.; Ganesan, S.; Nanayakkara, N. P. D.; Dias, L. R. S.; Walker, L. A. *Bioorg. Med. Chem. Lett.* **2012**, *22*(4), 1701.
10. (a) Song, M.-S.; Matveychuk, D.; MacKenzie, E. M.; Duchcherer, M.; Mousseau, D. D.; Baker, G. B. *Prog. Neuro-Psychoph.* **2013**, *44*, 118; (b) Zheng, H.; Amit, T.; Bar-Am, O.; Fridkin, M.; Youdim, M. B. H.; Mandel, S. A. *J. Alzheimer's Dis.* **2012**, *30*(1), 1.
11. Kalgutkar, A. S.; Dalvie, D. K.; Castagnoli, N.; Taylor, T. *J. Chem. Res. Toxicol.* **2001**, *14*(9), 1139.
12. Riederer, P.; Danielczyk, W.; Grünblatt, E. *Neurotoxicology* **2004**, *25*, 271.
13. (a) Luo, Z.; Sheng, J.; Sun, Y.; Lu, C.; Yan, J.; Liu, A.; Luo, H.-B.; Huang, L.; Li, X. *J. Med. Chem.* **2013**, *56*(22), 9089; (b) Luo, Z.; Liang, L.; Sheng, J.; Pang, Y.; Li, J.; Huang, L.; Li, X. *Bioorg. Med. Chem.* **2014**, *22*(4), 1355; (c) Su, T.; Xie, S.; Wei, H.; Yan, J.; Huang, L.; Li, X. *Bioorg. Med. Chem.* **2013**, *21*(18), 5830; (d) Lu, C.; Guo, Y.; Yan, J.; Luo, Z.; Luo, H.-B.; Yan, M.; Huang, L.; Li, X. *J. Med. Chem.* **2013**, *56*(14), 5843.
14. Youdim, M. B. H.; Amit, T.; Bar-Am, O.; Weinreb, O.; Yogev-Falach, M. *Neurotox. Res.* **2006**, *10*(3/4), 181.
15. Lu, C.; Zhou, Q.; Yan, J.; Du, Z.; Huang, L.; Li, X. *Eur. J. Med. Chem.* **2013**, *62*, 745.
16. Tran, K.-V.; Bickar, D. *J. Org. Chem.* **2006**, *71*(17), 6640.
17. Huang, L.; Liu, J.; Shan, W.; Liu, B.; Shi, A.; Li, X. *Chirality* **2010**, *22*(2), 206.
18. Hindo, S. S.; Mancino, A. M.; Braymer, J. J.; Liu, Y.; Vivekanandan, S.; Ramamoorthy, A.; Lim, M. H. *J. Am. Chem. Soc.* **2009**, *131*(46), 16663.
19. Youdim, M. B.; Edmonson, D.; Tipton, K. F. *Nat. Rev. Neurosci.* **2006**, *7*, 295.
20. (a) Ou, B.; Hampsch-Woodill, M.; Prior, R. L. *J. Agric. Food Chem.* **2001**, *49*(10), 4619; (b) Dávalos, A.; Gómez-Cordovés, C.; Bartolomé, B. *J. Agric. Food Chem.* **2003**, *52*(1), 48.
21. (a) Sharma, A. K.; Pavlova, S. T.; Kim, J.; Finkelstein, D.; Hawco, N. J.; Rath, N. P.; Kim, J.; Mirica, L. M. *J. Am. Chem. Soc.* **2012**, *134*(15), 6625; (b) Baum, L.; Ng, A. *J. Alzheimer's Dis.* **2004**, *6*(4), 367; (c) Geng, J.; Li, M.; Wu, L.; Ren, J.; Qu, X. *J. Med. Chem.* **2012**, *55*(21), 9146.
22. (a) Di, L.; Kerns, E. H.; Fan, K.; McConnell, O. J.; Carter, G. T. *Eur. J. Med. Chem.* **2003**, *38*(3), 223; (b) Camps, P.; Formosa, X.; Galdeano, C.; Muñoz-Torrero, D.; Ramírez, L.; Gómez, E.; Isambert, N.; Lavilla, R.; Badia, A.; Clos, M. V.; Bartolini, M.; Mancini, F.; Andrisano, V.; Arce, M. P.; Rodríguez-Franco, M. I.; Huertas, Ó.; Dafni, T.; Luque, F. J. *J. Med. Chem.* **2009**, *52*(17), 5365; (c) Wohnsland, F.; Faller, B. *J. Med. Chem.* **2001**, *44*(6), 923.